

NASA Technical Memorandum 89872
AIAA-87-9203

High Temperature Solid Oxide Regenerative Fuel Cell for Solar Photovoltaic Energy Storage

(NASA-TM-89872) HIGH TEMPERATURE SOLID
OXIDE REGENERATIVE FUEL CELL FOR SOLAR
PHOTOVOLTAIC ENERGY STORAGE (NASA) 19 P
Avail: NTIS HC A02/MF A01 CSCL 10C G3
11/44 0074229
N87-23020
Unclas

David J. Bents
Lewis Research Center
Cleveland, Ohio

Prepared for the
22nd Intersociety Energy Conversion Engineering Conference
cosponsored by the AIAA, ANS, ASME, SAE, IEEE, ACS, and AIChE
Philadelphia, Pennsylvania, August 10-14, 1987

NASA

David J. Bents
National Aeronautics and Space Administration
Lewis Research Center
Cleveland, Ohio 44135

Abstract

This paper describes a hydrogen-oxygen regenerative fuel cell (RFC) energy storage system based on high temperature solid oxide fuel cell (SOFC) technology. The reactants are stored as gases in lightweight insulated pressure vessels. The product water is stored as a liquid in saturated equilibrium with the fuel gas. The system functions as a secondary battery and is applicable to darkside energy storage for solar photovoltaics.

The system design, its component parts and their arrangement is presented. Forward and reverse operating cycles are described. Since the RFC is most applicable to operating regimes where reactant storage dominates system weight, the system uses the SOFC high temperature properties not to reduce radiator size but minimize reactant storage instead. Heat flow, mass, and energy balances are presented to characterize system operation and show how internal state and performance varies as reactant storage pressure rises and falls. Based upon these calculations, established mass models of the better-known system components, and the currently accepted projections for SOFC stack characteristics, the size and weight of this system is estimated over the range 10 to 300 kWe, for charge/discharge cycles up to 30 days duration (charging period roughly equal to or greater than the discharging period). Near-term aerospace SOFC technology (Argonne National Laboratory's Mod. 0 monolith) is used as the basis for characterization.

For solar PV application over the range investigated the system appears to be superior to alkaline RFC's and also quite competitive with advanced technology batteries and nuclear sources; demonstrating superior specific weight in the intermediate mission range of 3 to 72 hr darkside. Specific weight improves as charge/discharge time increases; the system weighs less than nickel hydrogen battery systems after 0.7 hr darkside, maintaining a specific weight advantage over radioisotope thermal generators (RTG's) for discharge periods up to 72 hr.

Introduction

Solid oxide fuel cell technology is of interest to space power system developers because, if this technology is developed, its novel characteristics offer system-enabling capabilities not available from the more well-established fuel cell types. These capabilities include high power density (up to 8 W/cm² of stack is claimed), reduced internal resistance etc. resulting from the small cell dimensions, one piece construction from thin multiple layers of ceramic (hence the term "monolithic"), and direct waste heat removal by the reactant streams at elevated temperature (1000 °C); leading to reduced radiator size, simplified reactant and thermal management. The

SOFC shares the same fundamental electrochemistry, thermodynamics of the better-known low temperature fuel cell technologies, but its solid state and faster kinetics should render it much less sensitive to variations in reactant composition, contaminants; thereby leading to system designs that are rugged, more compact, and less complicated. For energy storage RFC systems these characteristics translate to greater integration flexibility, resulting from a wider range of temperatures, pressures to work with for balancing flow, heat exchange during the optimization process for that particular application. Compared to the alkaline RFC,¹ the novel operating characteristics of SOFC's appear to confer system level advantages for energy storage which make it more attractive.

Consider the RFC system shown in Fig. 1, designed to provide darkside energy storage for solar photovoltaic (PV) power. For space this is one of the most important applications since, with PV, the secondary battery is an indispensable element; there are inevitable sun/shade cycles for almost all missions of interest. A remote terrestrial (or Mars surface) energy storage system is used to illustrate the basic design; however, the cycle description and system characterization can be extended to all darkside applications.

System Description

The major elements of this system are the converter unit, storage tanks (for oxygen, the fuel gas, and product water), and a radiator. The storage tanks are pressure vessels; moderately insulated and of lightweight composite construction. The converter unit, fuel tank, and oxygen tank are connected together through hoses and are all at the same pressure (which ranges from 5 to 100 atm). For sustained operating periods such as Mars or lunar night the converter and storage reservoirs are separate; for applications covering shorter discharge periods a single pressure vessel might be used to enclose all three.

The fuel storage reservoir contains a saturated mixture of hydrogen gas and vapor and includes a sump for product water accumulation. Within its interior, connected through external hoses and wiring harness, are temperature, pressure, and relative humidity sensors, a fuel gas intake/outlet standpipe and a thermal control radiator. Water vapor content within the tank is maintained at about 10 mol % by the release of controlled amounts of waste heat to its interior.

The oxygen tank is similar in form and equipment. It contains the (stoichiometric) amount of pure oxygen matching the fuel gas' hydrogen content. The stored gas is dry. The oxygen tank is connected to the converter unit by a pressurized hose for reactant gas transport, plus two fluid hoses for thermal transport (the fuel tank connection includes a third liquid hose for product water transport).

The converter is a sealed unit depicted schematically in Fig. 2. Within the converter there is a high temperature section (SOFC stack and reactant preheat heat exchangers) surrounded by insulation, and a low temperature section (gas flow and fluid transport). The stack functions as both an electrolyzer and a fuel cell. Similar to alkaline RFC systems, the stack is combined with a recirculating loop that removes product water and adds more fuel gas to the stream as hydrogen is consumed. A condenser combined with mechanical pump/separator is used to remove the water. Compared to the alkaline RFC, however, this recirculating loop operates at higher temperature, lower utilization, and a much higher flow rate per kilowatt since the fuel gas stream also removes the stack waste heat.

Converter High Temperature Section

Within the high temperature section, the SOFC stack is the element where electrochemical conversion actually takes place. It operates at 1273 K (1000 °C). It is a thinwall corrugated ceramic structure that in the Mod 0 embodiment (Fig. 3) resembles a compact crossflow heat exchanger. The stack is a bipolar array of individual fuel cells; the cells are sandwiched layers of alternating flat and corrugated thin sheets, sintered together to form a single piece that contains the entire array and all the individual cell elements (anode, electrolyte and cathode layers, the bipolar interconnects), which are themselves multilayer laminations of different ceramic materials which form the active cell components. In the ANL Mod 0 stack configuration the sandwiched corrugations are stacked at right angles to each other, forming alternating passages for fuel gas and oxygen so that the individual cells are parallel in flow but connected electrically in series. The passages for fuel gas are open at both ends to allow the recirculating stream to pass through the stack; the oxygen passages are open at only one end.

The stack is bordered on four sides by two separate sets of reactant preheat heat exchangers (RPHX's) for the oxygen and fuel gas streams; a manifold that splits the exhaust flow between them, and a plenum directing the fuel gas preheat exhaust stream around the oxygen side which is "dead-ended." Figure 4(a) shows the RPHX stack integration; Fig. 4(b) shows exhaust flow pattern through these heat exchangers. They control heat loss from the stack and reduce the inlet temperature gradient it must withstand. All heat exchangers are counterflow. Each HX is split into two separate sections which are constructed of different materials according to the reactants and temperature ranges experienced. The RPHX section No. 1 for fuel gas also contains a feed-water heater/boiler ("steam leg") for condensate. Temperatures at the inlet and exit side of the RPHX can range from 355 to 750 K; next to the stack they vary from 973 to 1273 K.

The stack is also bordered top and bottom by metal current collector plates which contact the ceramic monolith stack through pads of nickel felt. The entire high temperature section (stack, heat exchangers, and contacts) is surrounded by a substantial blanket of insulation to reduce stack temperature gradient, heat loss, and protect the low temperature components within the converter.

Low Temperature Section

The low temperature section contains the waste heat and water removal portion of the recirculating loop. Temperatures in this section range from less than 300 K, within the condenser cooling loop when electrolysis begins, to 750 K at the condenser inlet during fuel cell operation. However, the pumps, valves, metering, and other mechanical components are located downstream where operating temperatures no greater than 450 K are experienced.

The pump/separator circulates the fuel gas. It provides enough pressure drop to allow flow to be diverted to and from the storage reservoir by proportional control valves located at the pump inlet and exit. On the other hand, oxygen flow is not mechanically pumped but driven by concentration gradient only.

The condenser is cooled by a pumped fluid loop that circulates through internal radiators in both pressure vessels before it reaches the main radiator. This thermal management system ultimately removes the stack waste heat and controls internal temperature, acting to maintain the desired (10 mol % saturation) moisture content within the recirculating fuel gas and storage tank. Condenser exit temperature is controlled by modulating coolant flow (pump speed); internal radiator heat loads are separately adjusted via bypass. Waste heat, initially rejected by the stack at high temperature, is distributed throughout the system at a lower temperature via the condenser, finally exiting the system through the tank walls as well as the radiator. This system does not take advantage of the SOFC stack high temperature heat rejection capability to minimize radiator size, but condenses the product water to minimize reactant storage instead.

System Operation

The system operates like a secondary battery. It accumulates hydrogen and oxygen gas through vapor electrolysis during periods of sunlight, and discharges electricity during periods of darkness through (fuel cell) consumption of these reactants. All energy for the electrolysis cycle is supplied by the photovoltaic array.

At the beginning of electrolysis most of the hydrogen and oxygen is liquid water at the bottom of the sump. Pressure inside the system is low (for the analysis it is 5 atm). When the electrolysis cycle is complete the reactants are gases at somewhat higher temperature, and greatly increased pressure (100 atm, due to fixed storage volume). This situation reverses itself during (darkside) forward operation as hydrogen and oxygen gas are reacted to form steam and then condensed. The fuel gas is not pure hydrogen but contains some water vapor; a consequence of incomplete electrolysis but also necessary to maintain reducing atmosphere in the fuel gas stream. Typically at least 10 mol % water vapor is required. To maintain vapor partial pressure corresponding to 10 mol %, storage and condenser exit temperatures are controlled to track internal pressure along the (10 mol %) saturation line as it rises and falls. This temperature, which is also an indicator of reactant accumulation/depletion

within the system, is essentially an equilibrium temperature since it changes relatively slowly with time.

Regenerative Operation

For purposes of analysis the electrolysis cycle begins at the sump. Liquid water at equilibrium temperature is pumped into the steam leg of the RPHX section No. 1, heated, and vaporized. The saturated vapor mixes adiabatically with the recirculating fuel gas stream (10 mol % water vapor mixed with hydrogen slightly heated above saturation) and is further heated in RPHX section No. 2. The superheated steam/hydrogen mixture leaves this section and enters the stack at approximately 1000 K. Vapor content is approximately 30 percent.

When the stack acts as an electrolyzer, water vapor in the recirculating stream is reduced to hydrogen and oxygen is formed in a separate stream. Energy for the electrolysis process is externally supplied. Voltage applied to the stack must overcome not only the electrochemical potential but also cell resistance and polarization losses. As a result, some waste heat is also produced in addition to the reprocessed reactants. In this system waste heat is used to vaporize and superheat the water before it is reprocessed; consequently a minimum, rather than a maximum, energy loss requirement is imposed on the electrolyzer. For example, the waste heat required to sustain condensate vaporization at 5 atm would be equivalent to 400 mV of loss; at 100 atm only 220 mV would be needed. Fortunately, electrolysis polarization losses for SOFC appear to be well within this range.² Table 1 summarizes single cell performance when the stack operates as an electrolyzer.

The reprocessed fuel gas and oxygen streams leave the stack at 1273 K and enter their respective RPHX's. Both streams lose some heat to the recirculating inlet gas in RPHX section No. 2, but most heat transfer takes place in section No. 1 where the condensate is vaporized. Final temperature of the reprocessed gas exiting the RPHX is 30 to 50 K above the recirculating stream and liquid water that entered initially.

The oxygen stream is pumped by positive concentration pressure gradient from the converter into its storage tank where it loses heat to the surroundings until equilibrium temperature is reached. The fuel gas stream on the other hand is drawn through the condenser, where it loses heat until its temperature is stabilized at equilibrium. It is then drawn into the pump/separator, which forces it through a proportioning valve that shunts a fraction of the recirculating flow to storage. The remaining flow continues in the recirculating stream.

Figure 5 shows state points, temperature, and flow distribution within the converter at the beginning of electrolysis. As the electrolysis cycle proceeds and more reactant gas is reprocessed, the system internal pressure slowly rises until it reaches 100 atm at the end of the cycle. Table 2 summarizes the change in converter performance, state points as internal pressure rises from 5 to 100 atm.

Forward Operation

Fuel cell operation begins at the RPHX. Recirculating fuel gas and oxygen streams enter the RPHX at equilibrium temperature. There they are heated by the (recirculating return) exhaust gas to 973 K before they enter the stack.

When the stack acts as a fuel cell, reactants are converted to water vapor accompanied by the release of electrical energy and heat. The oxygen passages within the stack are "dead-ended;" that is, all the oxygen admitted to the stack is consumed. The recirculating fuel gas stream, on the other hand, passes through the stack losing only a fraction of the hydrogen it contains. As fuel gas passes through the stack, hydrogen is consumed and replaced with water vapor. The net effect is to lower the hydrogen content and increase the vapor content. Vapor content at the stack exit is approximately 30 percent, which translates to a net change, or cell utilization, of approximately 25 percent. Table 3 shows single cell performance (cell voltage, inlet and exit molar concentrations, thermal efficiency etc.) during stack forward operation. All of the waste heat produced by the stack is rejected to the recirculating steam, which experiences an approximately 300 K temperature rise to 1273 K at the stack exit. When the stream flows back out through the RPHX as exhaust, about half this waste heat is given up to the incoming reactants, cooling the exhaust to approximately 700 K before it reaches the condenser.

The condenser cools the exhaust to equilibrium temperature; from a mixture of super heated steam and hydrogen at the condenser inlet to a saturated mixture of hydrogen gas, water vapor, and liquid at the condenser exit. Condensation reduces the products of reaction to their most compact form, removing not only the waste heat remaining from fuel cell operation but also the heat of vaporization introduced earlier during the electrolysis cycle.

The saturated hydrogen/vapor/liquid is drawn out of the condenser by the pump/separator downstream. Makeup fuel gas from storage is introduced at the pump inlet through an admission valve, resulting in increased hydrogen flow but no change in molar composition. The pump/separator removes liquid entrained in the stream and sends it to the sump, while the gas continues to recirculate.

Figure 6 shows state points, temperature, and flow distribution within the converter at the beginning of forward operation. As the reactant gas is consumed, internal pressure slowly drops. Table 4 summarizes converter internal state and performance as the pressure falls from 100 to 5 atm.

System Characterization

The RFC system described here can be characterized on the basis of its conceptual design and operating cycles in order to establish a preliminary estimate of size and weight. This estimate is not a competitive evaluation pitting new technology against existing RFC systems but is an assessment of the new technology gauging its

potential if successfully developed. The SOFC has not yet matured to the point where large stack arrays can be produced (arrays up to 5 kWe have been tested but the ANL monolith considered by this analysis has only been built in sizes up to a few watts) but it is nonetheless possible to make performance estimates for larger arrays now due to the modular nature of the SOFC stack and individual cell performance which has already been demonstrated.³ These array performance extrapolations can be used to estimate overall performance and characteristics of the SOFC regenerative fuel cell because the other system components have been well-characterized; i.e. they are well enough understood that there is widespread agreement concerning their basis of estimation, modeling methodology. System designs configured for the end user are required early on for characterization, because they indicate whether or not the technology is worth developing for that application.

Based upon the operating cycle previously described, established mass models of the better known system components, and the currently accepted projections for SOFC stack characteristics, the size and weight of the various system components was estimated over the range of output power levels 10 to 300 kWe, and tabulated together to compose an overall estimate for the system, for charge/discharge cycles up to 500 hr duration.

An example tabulation of the system component weights for a 10 kWe Mars surface combined solar PV/regenerative fuel cell power system appears in Table 5. Assumptions exerting influence on overall system weight that were not directly coupled into the cycle performance analysis were:

Pressure Vessel Shell and Insulation Materials

The storage tanks and converter structure/containment pressure vessel shells were assumed to be of laminated wound graphite filament/polyamide stressed to 25 ksi. One centimeter of multifoil insulation, 0.11 gram/cc, was included for interior lining. Design pressure was 100 atm.

SOFC Stack Size and Weight

The ANL Mod 0 monolith described in Refs. 3 and 4 was used. Key parameters are given in Table 6.

Radiator Size and Weight

All radiators were pumped fluid loop, aluminum platecoil construction, specific weight of 5.8 kg/m² of surface area. The external radiator would be physically equivalent to the main radiator used by the alkaline RFC.¹ For lunar and planetary darkside heat rejection a background temperature of 20 K was assumed. Emissivity was 0.72. Due to the low (~300 K) rejection temperature at the lowest pressure, the external radiator turned out to be roughly as large as the converter unit itself.

Solar PV Collectors

The PV collector mass listed in Table 5 and shown also in Fig. 7 was based on the technology assessment of Ref. 5; approximately 50 percent

solar flux reduction on Mars surface compared with Earth⁶ was also considered, resulting in an assigned value of 100 electrical watts per kilogram of solar array. The collector assembly was included as part of the overall power system shown in Figs. 1, 7, and Table 5 but was not included in the RFC comparisons with other darkside energy storage systems shown subsequently.

Heat Exchangers

Heat exchanger assumptions were not a significant influence on converter weight. For a fuel cell system, the heat loads are equivalent to only a fraction of the electrical power transfer, and the operating cycle maintains stream-to-stream temperature differences greater than 30 K everywhere. Using conservative values of mean effective heat transfer, heat exchanger packing density and specific weight, the combined weight of all heat exchangers remained less than 40 percent of the stack weight.

Figure 7 shows graphically how the weight of the major elements for a 10 kWe system (Table 5), including the PV array, changes as a function of the mission (darkside) time over the specified range. The analysis assumes that the daylight, or recharge time available is roughly equal to, or greater than, the discharge time. If the PV array is removed, the remaining system weight can be attributed to darkside energy storage, which is characterizable as a secondary battery and can be directly compared to other forms of energy storage.

Figure 8 presents specific weight, kilograms per kilowatt delivered, of the energy storage system alone over the range 1 to 500 hr, for design power levels of 10, 30, 100, and 300 kWe. Superimposed are (diagonal) lines of constant watt-hours per kilogram, an accepted universal figure of merit. Some established SOA values for commonly known storage technologies are: nickel-hydrogen battery systems, 33 W-hr/kg; solid metal flywheel rotors, 18 W-hr/kg and so on. The curve shape indicates a mass penalty associated with the fixed converter and radiator weight for short duration missions, but a benefit at longer mission times where reactant storage is a major component of the overall system. This can be attributed to the relatively high energy available from hydrogen/oxygen.

Figure 9 presents the same specific weight curve but overlays it with equivalent specific weight curves for three "rival" darkside energy storage systems within the same specified range. The electrochemical systems are selected for the comparison because they are presently deemed to be most competitive for the space PV darkside application. A constant slope of 33 W-hr/kg is superimposed representing SOA nickel-hydrogen battery systems. A constant slope of 100 W-hr/kg represents the advanced battery technology capability which may be achieved by high temperature sodium-sulfur battery systems.⁷ The "minimum mass integrated system" alkaline regenerative fuel cell of Ref. 1 is also superimposed since it is similar, with a converter weight that is fixed and pressurized gas reactant storage that cycles between 4 and 20 atm. Comparison is also made with nuclear sources. For sun/shade cycles approaching 100 hr, reactant storage dominates

system weight to such an extent that the mass of the PV array used for changing the system can be neglected. The RTG specific weight used to represent nuclear systems is the GPHS program goal of 5.2 kg/W⁸; this specific weight is also representative of a space reactor power system that uses a man-rated shield.

Results and Summary

The data show a clear region of interest for the high temperature solid oxide regen. fuel cell, where it exhibits much lower specific weight than the other systems shown. This region falls somewhere between the 2 and 70 hr sun/shade time; a time period out of the range of earth orbit applications, but well within the range of interest for Mars surface and remote terrestrial installations. On the other hand, lunar surface missions (327 hr of darkness) falls into the domain of nuclear generation unless the solid oxide fuel cell RFC was synergistic with other on-site hydrogen/oxygen systems, or there were compelling reasons not to use nuclear for a lunar base.

It therefore appears that, within the application we have defined, the high temperature solid oxide regen. fuel cell has the potential to be very competitive with several of the energy storage technologies now extant or under development.

References

- Hoberecht, M.A. and Rieker, L.L., "Design of a Regenerative Fuel Cell System for Space Station," Energy for the Twenty-first Century (20th IECEC), Vol. 2, SAE, 1985, pp. 2.202-2.207.
- Maskalick, N.J., "High-Temperature Electrolysis Cell Performance Characterization," Hydrogen Energy Progress V, T.N. Veziroglu and J.B. Taylor, eds., Pergamon Press, New York, 1984, pp. 801-812.
- Fee, D.C., et al., "Monolithic Fuel Cell Development," 1986 National Fuel Cell Seminar Abstracts, Courtesy Associates, Washington, D.C., 1986, pp. 40-43.
- McPheeters, C.C., et al., "Fabrication of a Solid Oxide Fuel Cell Monolithic Structure," 1986 National Fuel Cell Seminar Abstracts, Courtesy Associates, Washington, D.C., 1986, pp. 44-47.
- Scott-Monck, J., and P. Stella, "Current Status of Advanced Solar Array Technology Development," Energy for the Twenty-first Century (20th IECEC), Vol. 1, SAE, 1985, pp. 1.32-1.35.
- Glasstone, S., The Book of Mars, NASA SP-179, NASA, Washington, D.C., 1968.
- Rasmussen, J.R., "Development of an Advanced Sodium/Mixed Sulfur/Selenium Battery System for Space Power Applications," Energy for the Twenty-first Century, (20th IECEC), Vol.1, SAE, 1985, pp. 1.309-1.314.
- Rock, B.J., "Radioisotope Space Power Programs," Space Power, NASA CP-2351, NASA, Washington, D.C., 1984, pp. 75-84.

TABLE 1 - SINGLE CELL PERFORMANCE

[Electrolysis Operation.]

	Beginning		Fully charged
Operating pressure, atm	5	50	100
Inlet moisture content, mol %	27.2	31	32.5
Exit moisture content, mol %	10	10	10
Water utilization, percent	63.2	67.7	69.2
Applied voltage, V	1.525	1.525	1.525
Losses			
IR loss, mV	40	40	40
Polarization, mV	400	337	318
Reversible cell voltage, V	1.084	1.148	1.167
Stack inlet temperature, K	1048.5	1001.5	983
Stack exit temperature, K	1273	1273	1273

TABLE 2 - ELECTROLYSIS CYCLE SUMMARY

	Beginning		Fully charged
Internal operating pressure, atm	5	50	100
Operating temperatures, K			
Stack	1273	1273	1273
Recirculating stream, at:			
RPHX inlet	355	425	453
RPHX between			
numbers 1 and 2	382	473.5	512.5
Stack inlet	1048.5	1001.5	983
Stack exit	1273	1273	1273
RPHX exhaust between			
numbers 2 and 1	653	789	844
Condenser inlet	386	487.5	535.5
Condenser exit	355	425	453
Oxygen stream at:			
Stack outlet	1273	1273	1273
RPHX between			
numbers 2 and 1	653	789	844
RPHX exit	386	487.5	535.5
Radiator loop	305	375	403
Performance summary at 10 kWe			
Recirculating stream flow, liter/min	345.4	338.6	336.8
Water consumption, cc/mm	36.7	36.7	36.7
Hydrogen production, mol/hr	122.360	122.352	122.348
RPHX heat load, kWt			
Section number 1	1.72	1.64	1.58
Section number 2	4.19	2.76	2.30
Condenser heat load, kWt	0.18	0.33	0.41

TABLE 3 - SINGLE CELL PERFORMANCE

[Forward operation.]

	Beginning		Fully discharged
Operating pressure, atm	100	50	5
Stack inlet temperature, K	974	974.5	973.5
Stack exit temperature, K	1273	1273	1273
Inlet moisture content, mol %	10	10	10
Exit moisture content, mol %	32.5	31	27.2
Hydrogen utilization, percent	25	23.33	19.11
Reversible voltage, V	1.086	1.071	1.018
IR loss, mV	40	40	40
Output voltage, V	1.046	1.031	0.978

TABLE 4 - FORWARD CYCLE SUMMARY

[Fuel cell.]

	Beginning		Fully discharged
Internal operating pressure, atm	100	50	5
Operating temperatures, K			
Stack	1273	1273	1273
Recirculating stream, at:			
RPHX inlet	453	425	355
Stack inlet	974	974.5	973.5
Stack exit	1273	1273	1273
Condenser inlet	750	722	655.5
Condenser exit	453	425	355
Oxygen stream at:			
RPHX inlet	453	425	355
Stack inlet	974	974.5	973.5
Radiator loop	403	375	305
Performance summary at 10 kWe			
Recirculating stream flow, liter/min	490.9	500.7	538.4
Hydrogen consumption, mol/hr	178.30	180.93	190.74
Water production, cc/min	53.49	54.28	57.22
RPHX heat load, kWt	3.91	4.44	6.29
Condenser heat load, kWt	3.97	4.29	5.28

TABLE 5 - MARS SURFACE COMBINED SOLAR PV/HIGH
TEMPERATURE SOLID OXIDE REGENERATIVE
FUEL CELL
POWER SYSTEM SUMMARY AT 10 kWe

Power level (delivered)	10 kWe
Shade time assumed	13 hr
Sun time allowed	11 hr
Required solar PV daylight Power	29.9 kWe
Component breakdown	
Reactants and tankage	
Fuel gas	11 kg
Tank (1.32 m diameter sphere)	182 kg
Oxygen	42 kg
Tank (1.00 m diameter)	84 kg
Reactants and tankage total	319 kg
Converter unit (prism 50 cm diameter by 80 cm height)	
SOFC stack (10 by 10 by 46 cm)	20 kg
Reactant preheat HX's	5.3 kg
High temperature insulation package	6 kg
Condenser HX	1.5 kg
Low temperature section ancillaries	38 kg
Structure and containment	36 kg
Converter unit total	107 kg
External radiator	91 kg
Solar PV panel and mounts	300 kg
Total	817 kg

TABLE 6 - ANL MOD 0 MONOLITH SOFC PHYSICAL
AND PERFORMANCE PARAMETERS

Dimensions	
Cell height	2 mm
Flow length and stack width (crossflow configuration)	10 cm
Electrode layer thickness	0.25 mm
Electrolyte layer thickness	0.025 mm
Interconnect thickness	0.025 mm
Stack active surface to volume ratio	3.3 cm ² /cm ³
Active cell density	3.021 g/cm ³
Current density	500 ma/cm ²
Volumetric power density	1.6 W/cm ³
Specific weight	2 kg/kWe

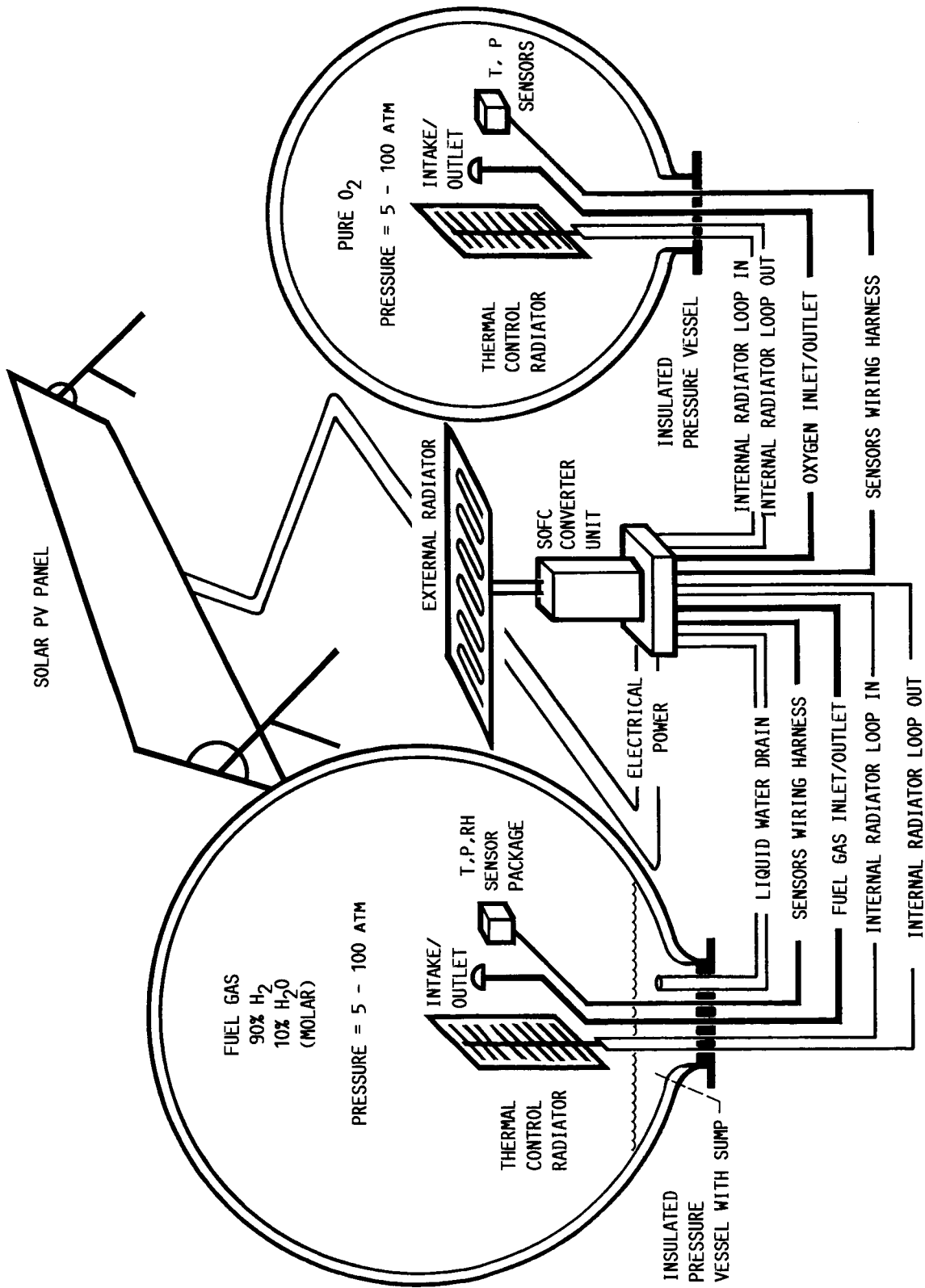


FIGURE 1. - SOLID OXIDE REGENERATOR FUEL CELL/SOLAR PV POWER SYSTEM.

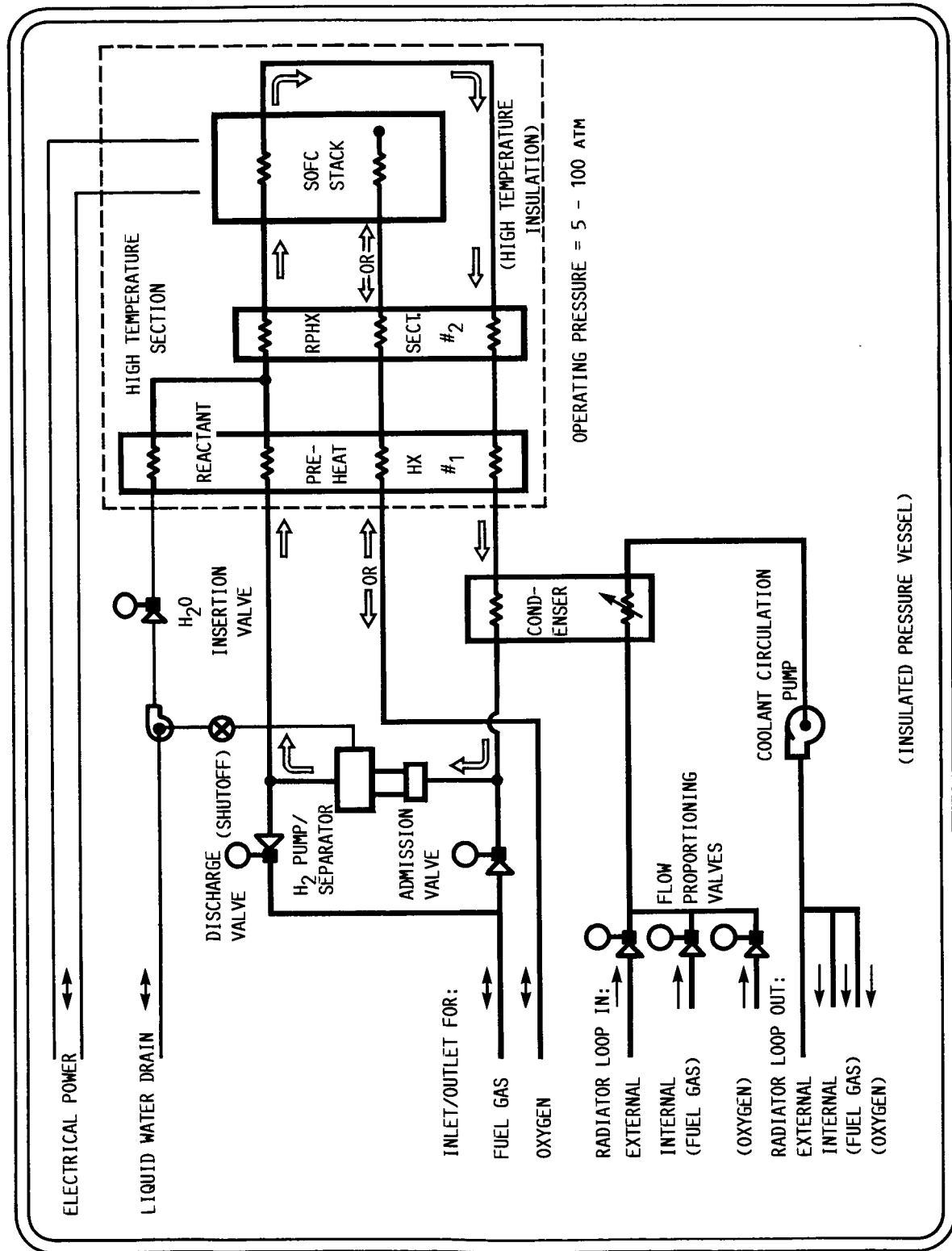


FIGURE 2. - CONVERTER UNIT DIAGRAM.

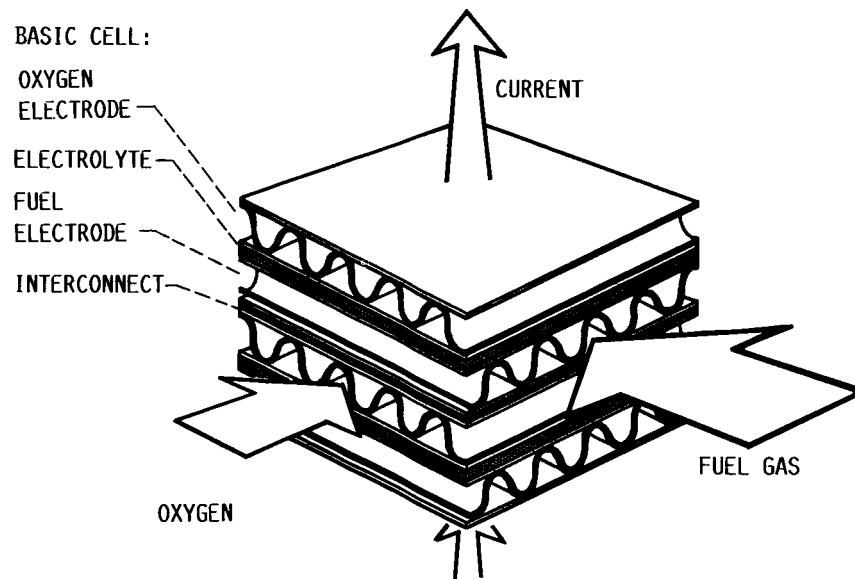
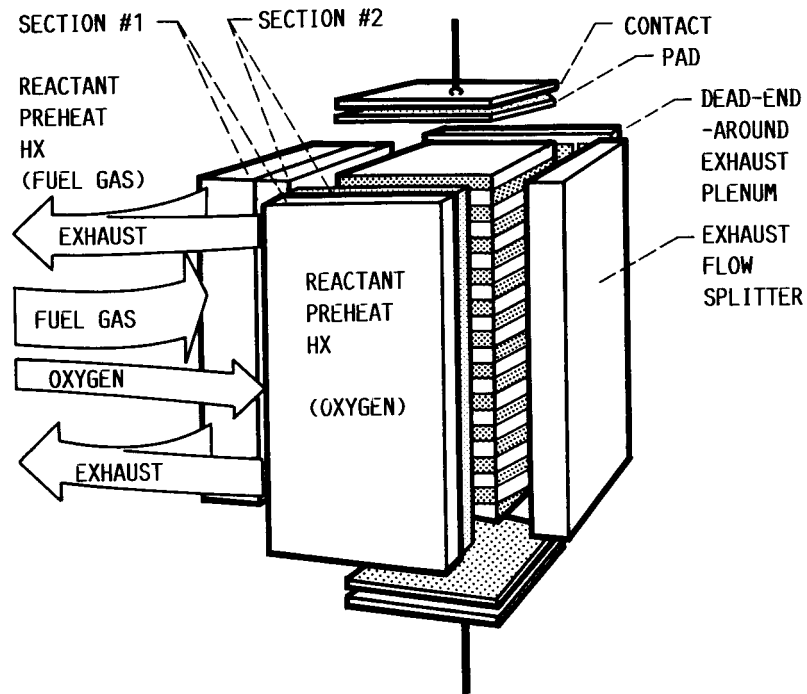
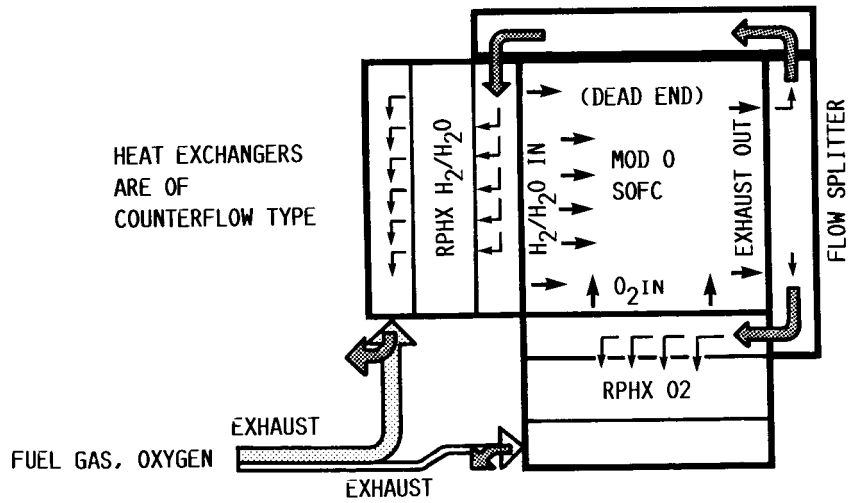


FIGURE 3. - ANL MOD. ZERO SOFC.



(A) INTEGRATION.



(B) FLOW PATTERN.

FIGURE 4. - STACK HEAT EXCHANGER.

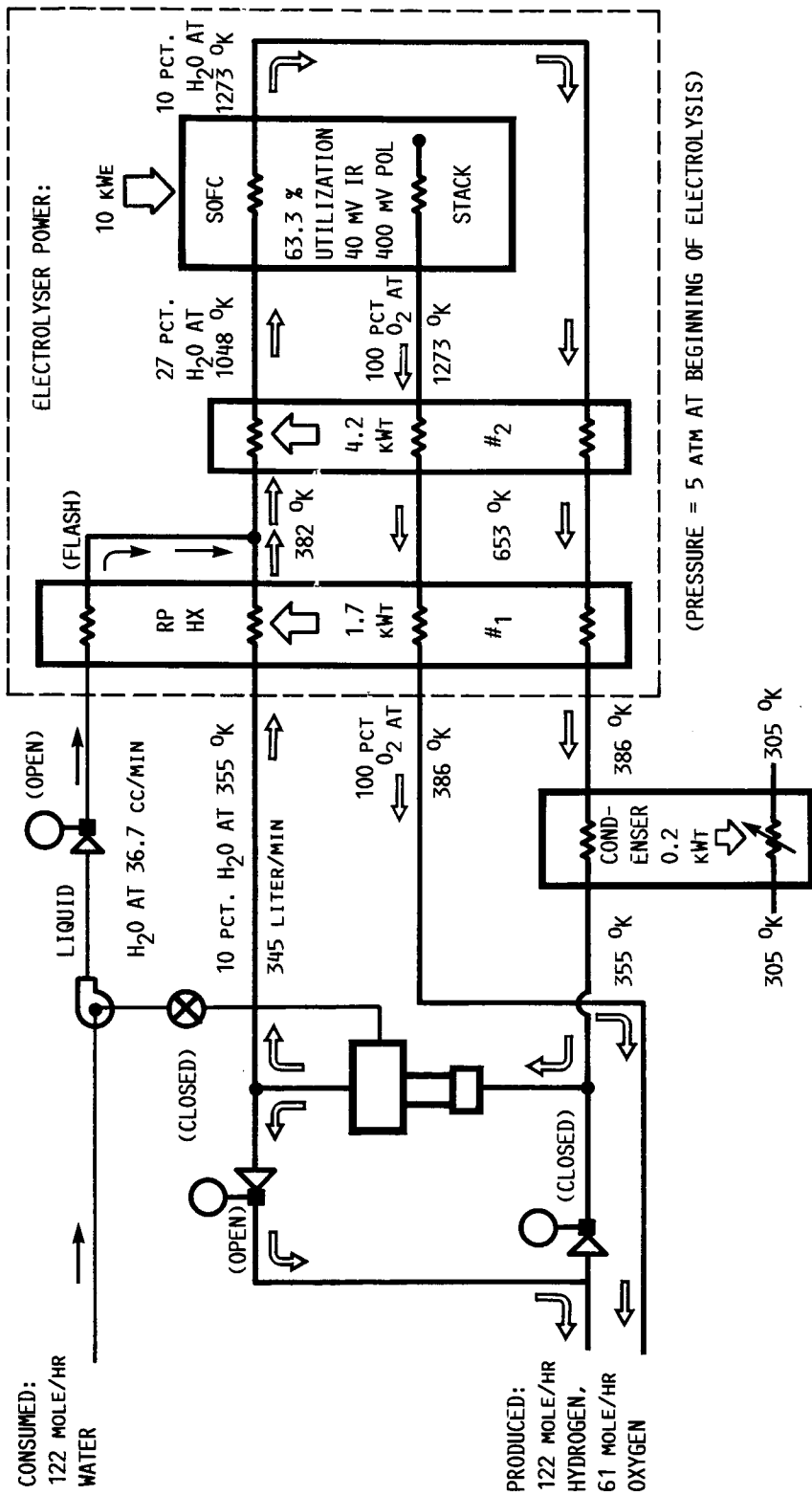


FIGURE 5. - TEMPERATURE AND FLOW DISTRIBUTION AT BEGINNING OF ELECTROLYSIS CYCLE.

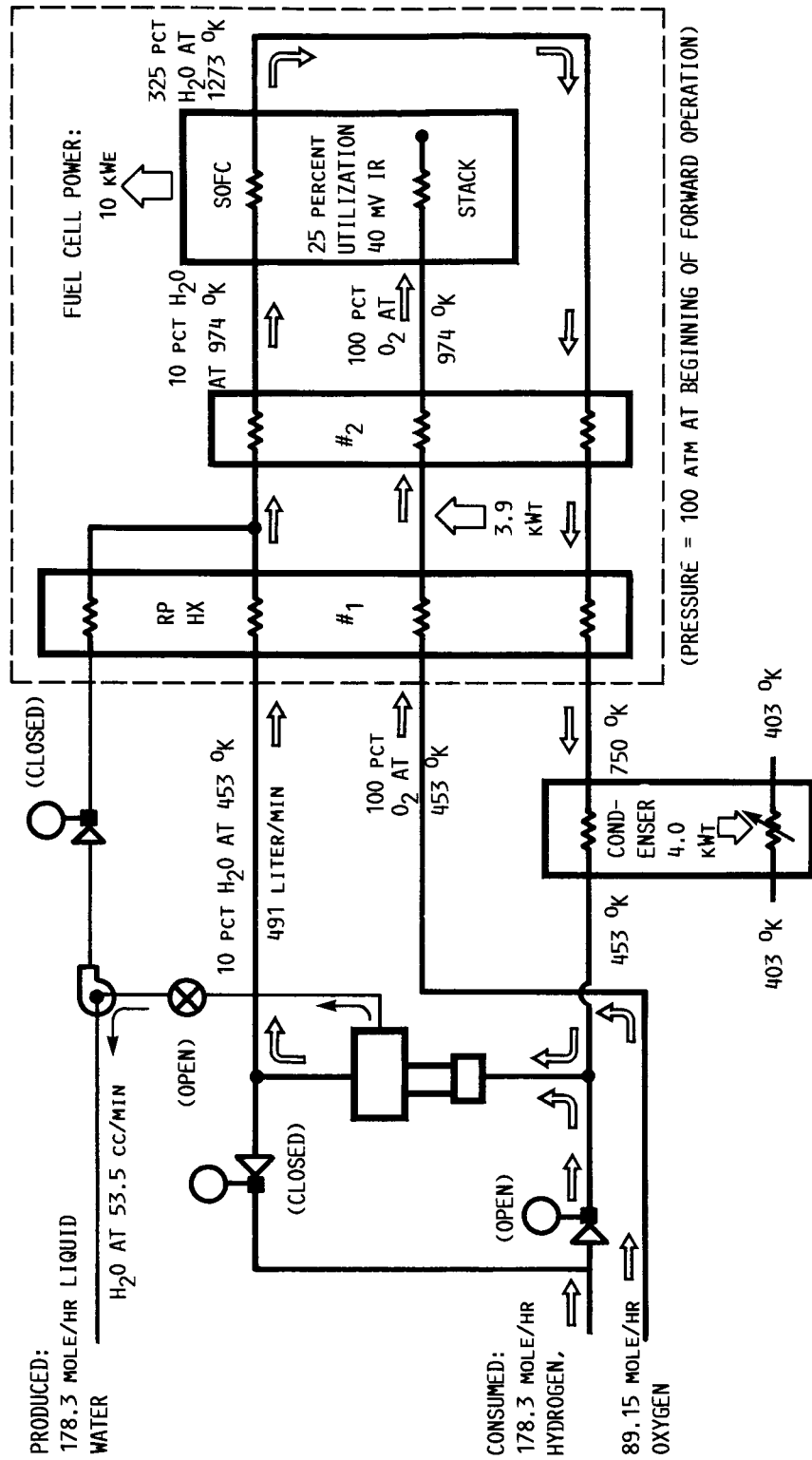


FIGURE 6. - TEMPERATURE AND FLOW DISTRIBUTION AT BEGINNING OF FORWARD (FUEL CELL) OPERATION.

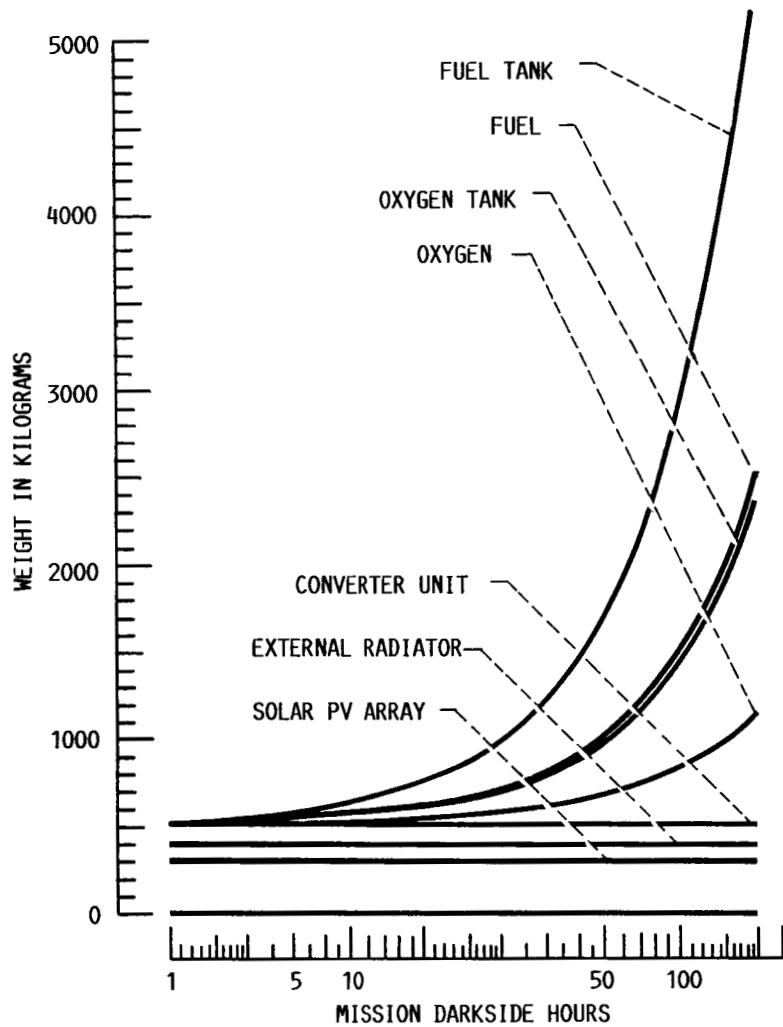


FIGURE 7. - COMBINED SOLAR PV/HIGH TEMPERATURE SOLID OXIDE REGENERATIVE FUEL CELL, MAJOR ELEMENT WEIGHT BREAKDOWN AT 10 KWE.

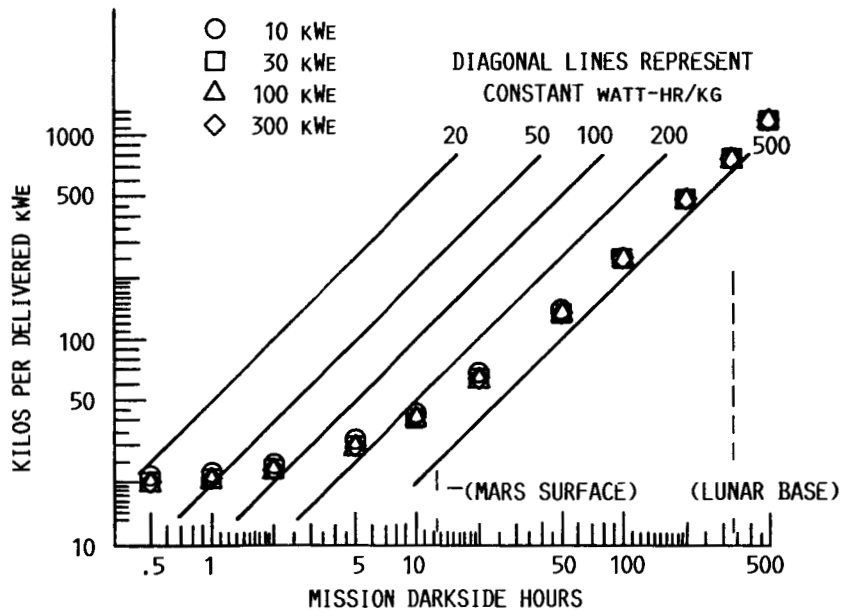


FIGURE 8. - HIGH TEMPERATURE SOLID OXIDE REGENERATIVE FUEL CELL ENERGY STORAGE SPECIFIC WEIGHT.

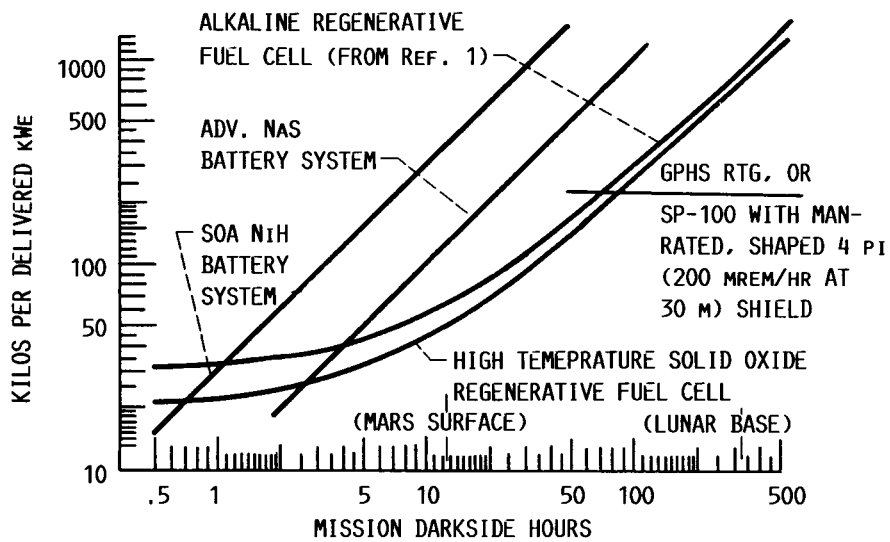


FIGURE 9. - HIGH TEMPERATURE SOLID OXIDE REGENERATIVE FUEL CELL SPECIFIC WEIGHT VERSUS COMPETITIVE DARKSIDE STORAGE.

1. Report No. NASA TM-89872 AIAA 87-9203		2. Government Accession No.		3. Recipient's Catalog No.	
4. Title and Subtitle High Temperature Solid Oxide Regenerative Fuel Cell for Solar Photovoltaic Energy Storage				5. Report Date	
				6. Performing Organization Code 506-41-31	
7. Author(s) David J. Bents				8. Performing Organization Report No. E-3549	
				10. Work Unit No.	
9. Performing Organization Name and Address National Aeronautics and Space Administration Lewis Research Center Cleveland, Ohio 44135				11. Contract or Grant No.	
				13. Type of Report and Period Covered Technical Memorandum	
12. Sponsoring Agency Name and Address National Aeronautics and Space Administration Washington, D.C. 20546				14. Sponsoring Agency Code	
15. Supplementary Notes Prepared for the 22nd Intersociety Energy Conversion Engineering Conference, cosponsored by the AIAA, ANS, ASME, SAE, IEEE, ACS, and AIChE, Philadelphia, Pennsylvania, August 10-14, 1987.					
16. Abstract <p>This paper describes a hydrogen-oxygen regenerative fuel cell (RFC) energy storage system based on high temperature solid oxide fuel cell (SOFC) technology. The reactants are stored as gases in light-weight insulated pressure vessels. The product water is stored as a liquid in saturated equilibrium with the fuel gas. The system functions as a secondary battery and is applicable to darkside energy storage for solar photovoltaics. The system design, its component parts and their arrangement is presented. Forward and reverse operating cycles are described. Since the RFC is most applicable to operating regimes where reactant storage dominates system weight, the system uses the SOFC high temperature properties not to reduce radiator size but minimize reactant storage instead. Heat flow, mass, and energy balances are presented to characterize system operation and show how internal state and performance varies as reactant storage pressure rises and falls. Based upon these calculations, established mass models of the better-known system components, and the currently accepted projections for SOFC stack characteristics, the size and weight of this system is estimated over the range 10 to 300 kWe, for charge/discharge cycles up to 30 days duration (charging period roughly equal to or greater than the discharging period). Near-term aerospace SOFC technology (Argonne National Laboratory's Mod 0 monolith) is used as the basis for characterization. For solar PV application over the range investigated the system appears to be superior to alkaline RFC's and also quite competitive with advanced technology batteries and nuclear sources; demonstrating superior specific weight in the intermediate mission range of 3 to 72 hr darkside. Specific weight improves as charge/discharge time increases; the system weighs less than nickel hydrogen battery systems after 0.7 hr darkside, maintaining a specific weight advantage over radioisotope thermal generators (RTG's) for discharge periods up to 72 hr.</p>					
17. Key Words (Suggested by Author(s)) Solid oxide fuel cells; Space power; Regenerative fuel cells; Fuel cell systems			18. Distribution Statement Unclassified - unlimited STAR Category 44		
19. Security Classif. (of this report) Unclassified		20. Security Classif. (of this page) Unclassified		21. No. of pages 17	22. Price* A02